Pergamon

Geochimica et Cosmochimica Acta, Vol. 64, No. 18, pp. 3085–3098, 2000

0016-7037/00 $20.00 + .00

PII S0016-7037(00)00397-5

Reduction of U(VI) in goethite (α-FeOOH) suspensions by a dissimilatory metal-reducing bacterium

JAMES K. FREDRICKSON,[1,*] JOHN M. ZACHARA,[1] DAVID W. KENNEDY,[1] MARTINE C. DUFF,[2] YURI A. GORBY,[1] SHU-MEI W. LI,[1] and KENNETH M. KRUPKA[1]

[1]Pacific Northwest National Laboratory, MSIN P7–50, P.O. Box 999, Richland, WA 99352, USA
[2]University of Georgia, Savannah River Ecology Laboratory, Aiken, SC 29802, USA

(*Received September* 8, 1999; *accepted in revised form March* 23, 2000)

Abstract—Dissimilatory metal-reducing bacteria (DMRB) can utilize Fe(III) associated with aqueous complexes or solid phases, such as oxide and oxyhydroxide minerals, as a terminal electron acceptor coupled to the oxidation of H_2 or organic substrates. These bacteria are also capable of reducing other metal ions including Mn(IV), Cr(VI), and U(VI), a process that has a pronounced effect on their solubility and overall geochemical behavior. In spite of considerable study on an individual basis, the biogeochemical behavior of multiple metals subject to microbial reduction is poorly understood. To probe these complex processes, the reduction of U(VI) by the subsurface bacterium, *Shewanella putrefaciens* CN32, was investigated in the presence of goethite under conditions where the aqueous composition was controlled to vary U speciation and solubility. Uranium(VI), as the carbonate complexes $UO_2(CO_3)^{4-}_{3(aq)}$ and $UO_2(CO_3)^{2-}_{2(aq)}$, was reduced by the bacteria to U(IV) with or without goethite [α-$FeOOH_{(s)}$] present. Uranium(VI) in 1,4-piperazinediethhanesulfonic acid (PIPES) buffer that was estimated to be present predominantly as the U(VI) mineral metaschoepite [$UO_3 \cdot 2H_2O_{(s)}$], was also reduced by the bacteria with or without goethite. In contrast, only ~30% of the U(VI) associated with a synthetic metaschoepite was reduced by the organism in the presence of goethite with 1 mM lactate as the electron donor. This may have been due to the formation of a layer of $UO_{2(s)}$ or $Fe(OH)_{3(s)}$ on the surface of the metaschoepite that physically obstructed further bioreduction. Increasing the lactate to a non-limiting concentration (10 mM) increased the reduction of U(VI) from metaschoepite to greater than 80% indicating that the hypothesized surface-veneering effect was electron donor dependent. Uranium(VI) was also reduced by bacterially reduced anthraquinone-2,6-disulfonate (AQDS) in the absence of cells, and by Fe(II) sorbed to goethite in abiotic control experiments. In the absence of goethite, uraninite was a major product of direct microbial reduction and reduction by AH_2DS. These results indicate that DMRB, via a combination of direct enzymatic or indirect mechanisms, can reduce U(VI) to insoluble U(IV) in the presence of solid Fe oxides.

1. INTRODUCTION

A variety of anaerobic bacteria can catalyze the reduction of soluble species of U(VI) to insoluble U(IV) forms. Some of these microorganisms, including those capable of S (Lovley et al., 1993) and Fe (Lovley et al., 1991) respiration, do so by a direct enzymatic process coupled to the oxidation of organic compounds or H_2 (Gorby and Lovley, 1992; Lovley and Phillips, 1992b). The product of this microbial reduction reaction is typically fine-grained uraninite [$UO_{2(s)}$] (Gorby and Lovley, 1992; Lovley and Phillips, 1992b). The formation of some uranium ore deposits is believed to involve direct microbial reduction of U(VI) (Lovley et al., 1991; Mohagheghi et al., 1985), as opposed to abiotic reduction by reduced species such as sulfide. Anderson, (1987) reported that U(VI) is not reduced to U(IV) by H_2S in anoxic seawater but rather diffuses into sediments where it is reduced to U(IV), possibly by anaerobic bacteria (McKee and Todd, 1993).

The purpose of this research was to investigate the reduction of U(VI), either as an aqueous species [$UO_2(CO_3)^{4-}_{3(aq)}$] or as metaschoepite [$UO_3 \cdot 2H_2O_{(s)}$], by the dissimilatory metal-reducing bacterium *S. putrefaciens* in the absence and presence of an Fe(III) oxide as an alternative electron acceptor during the metabolism of lactate. The influence of anthraquinone-2,6-disulfonate (AQDS) as a humic acid analog and electron shuttle (Lovley et al., 1998) on the microbial reduction process was investigated, as well as the potential for microbially generated reduced AQDS (AH_2DS) and Fe(II) to directly reduce U(VI). Soluble and extractable forms of U(VI) were measured and U X-ray absorption near edge structure (XANES) spectroscopy was used to determine the oxidation state of U associated with the solid phase and to quantify microbial reduction of U in complex mineral suspensions.

In addition to bacteria having an important role in the biogeochemical cycling of U, microbial processes can remove and concentrate U from contaminated ground and surface waters (Lovley and Phillips, 1992a) or from contaminated soil wash through reductive precipitation (Phillips et al., 1995b). Remediation of contaminated groundwater via wells and treatment ex situ is a relatively inefficient and costly process, while microbial U(VI) reduction can potentially be applied for the removal of U from solution in situ (Lovley, 1995).

Some DMRB can reduce solid phase Fe(III) oxides and oxyhydroxides including poorly crystalline phases such as ferrihydrite and crystalline phases such as goethite (Roden and Zachara, 1996), hematite (Zachara et al., 1998), and magnetite (Kostka and Nealson, 1995; Dong et al., 1999). *S. putrefacien*s

* Author to whom correspondence should be addressed (jim.fredrickson@pnl.gov).

and *S. algae* species appear to be particularly effective at reducing crystalline Fe(III) oxide phases although, to our knowledge, a systematic analysis of the ability of different DMRB to reduce different Fe(III) oxide minerals has not been undertaken. Fe(III) oxides are ubiquitous in nature and, in some aquifer sediments, they comprise the largest mass of oxidant (e.g., electron acceptor) for microbially catalyzed oxidation of organic compounds (Heron et al., 1994b). Hence, in Fe(III) oxide containing subsurface sediments with soluble U(VI), DMRB are presented with multiple electron acceptors that can be potentially linked to respiration. The actual $p\epsilon$ where the valence transformations occur is strongly dependent on pH, reactant concentrations, aqueous speciation, and solid-phase distribution of the elements, and chemical potentials of reactants and products formed. In oxidized soils and sediments at circumneutral pH, Fe(III) is typically present as insoluble (hydr)oxides, while a significant fraction of the total U(VI) can be soluble carbonate or hydroxo complexes. From a thermodynamic standpoint (Francis et al., 1994) and because of much greater solubility, U(VI) should be reduced preferentially to Fe(III), which is poorly soluble in the oxidized form. However, differences in bacterial enzyme specificity and kinetics make it difficult to predict the sequence of reduction. Also, on a mass basis, Fe(III) is typically present in much higher concentrations than U. Therefore, it is difficult to predict, a priori, the fate of U(VI) in Fe(III) oxide containing sediments as microbial metal reduction proceeds.

Uranium may exist in contaminated soils in a variety of valence states (predominantly IV and VI) reflecting the nature of the source term and weathering extent (Hunter and Bertsch, 1998; Morris et al., 1996). Uranium(VI) is the most stable valence form under oxidizing geochemical conditions (Grenthe et al., 1992a; Langmuir, 1978). While U(VI) precipitates in sparingly soluble mineral phases including metaschoepite [$UO_3 \cdot 2H_2O_{(s)}$] and various phosphates and silicates (Grenthe et al., 1995; Langmuir, 1978), $UO^{2+}_{2(aq)}$ forms a series of strong aqueous complexes with CO^{2-}_3 [e.g., $UO_2CO^o_{3(aq)}$, $UO_2(CO_3)^{2-}_{2(aq)}$, $UO_2(CO_3)^{4-}_{(aq)}$] that greatly enhance U(VI) solubility in carbonate containing waters at circumneutral pH and above. Uranium(VI)–carbonate aqueous complexes are neutral or anionic in charge, and poorly reactive with mineral surfaces such as Fe(III) and Al oxyhydroxides (Duff and Amrhein, 1996; Hsi and Langmuir, 1985; Waite et al., 1994) and clays that typically control metal ion migration in soil and groundwater by adsorption reactions. Remediation technologies for U(VI) contamination often involve reduction of mobile U(VI) aqueous complexes to insoluble U(IV) precipitates (Fiedor et al., 1998; Gu et al., 1998), where carbonate complexation has minimal effect on solubility (Casas et al., 1998). To be effective in the long term, however, remediation techniques for U(VI) must target both mobile aqueous species that are groundwater contaminants, as well as U(VI) precipitates that may be long term sources.

2. EXPERIMENTAL PROCEDURES

2.1. Bacteria, Media, and Minerals

S. putrefaciens strain CN32 was provided courtesy of Dr. David Boone (Subsurface Microbial Culture Collection, Portland State University, Portland, OR, USA). Strain CN32 was isolated from a subsurface core sample (250 m beneath the surface) from the Morrison Formation, a formation mined extensively for uranium, during drilling of a shale–sandstone sequence in northwestern New Mexico (Liu et al., submitted). CN32 was routinely cultured aerobically in tryptic soy broth (TSB), 30 g/L (Difco Laboratories, Detroit, MI, USA), and stock cultures were maintained by freezing in 40% glycerol at −80°C.

Solutions were buffered (pH ~ 7) with either $NaHCO_3$ or 1,4-piperazinediethanesulfonic acid (PIPES), at 30 mM. Sodium lactate was added as the electron donor and, in select treatments, AQDS (Sigma, St. Louis, MO, USA) was added separately. Lactate was used at 1 mM in most experiments and 10 mM in several cases. Medium was dispensed into pressure tubes, purged with N_2:CO_2 (80:20) for $NaHCO_3$-buffered medium or N_2 for PIPES-buffered medium and sealed with thick butyl rubber stoppers.

CN32 cells were harvested at mid to late log phase by centrifugation from TSB cultures, washed with buffer to remove residual medium, resuspended in $NaHCO_3$ or PIPES buffer, and purged. Cells were added to buffers to obtain a final concentration of 2 to 4×10^8 cells/mL.

A medium surface area goethite (52.3 m^2/g) was prepared by hydrolysis of Fe(III) solutions and aging at elevated temperatures according to Schwertmann and Cornell (1991). The precipitates were extracted three times with acidified hydroxylamine hydrochloride to remove any residual ferrihydrite, washed repeatedly to remove extractants, extensively dialyzed against deionized distilled H_2O and lyophilized. Metaschoepite [$UO_3 \cdot 2H_2O_{(s)}$] was synthesized by hydrolysis of a 0.01 mol/L $UO_2(NO_3)_2 \cdot 6H_2O$ solution by using methods described by Sowder et al. (1996) and characterized by XRD and high resolution transmission electron microscopy (HRTEM). Metaschoepite was maintained as an aqueous suspension in 10 mM PIPES, pH 7, until used.

2.2. Bacterial Reduction Experiments

The ability of *S. putrefaciens* strain CN32 to reduce U(VI), as U acetate or as metaschoepite, was evaluated in the presence or absence of 50 mM goethite. Goethite slurries were made to 250 mM in water and sonicated for 1 h to disperse the lyophilized particles. In a typical experiment with 10 mL final volume, 2 mL of goethite slurry was added to replicate pressure tubes, followed by 4.5 mL of 60 mM PIPES or $NaHCO_3$ buffer, 0.1 mL of 100 mM lactate, and 1.4 mL of deionized water. Tubes were purged with N_2 (PIPES) or N_2(80):CO_2(20) ($NaHCO_3$) and sealed with thick butyl rubber stoppers. One mL of CN32 cell suspension was added from a freshly washed culture of between 2 and 4×10^9 cells/mL in either 30 mM PIPES or $NaHCO_3$ by using a needle and syringe purged with N_2 or N_2:CO_2. One mL of anaerobic 10 mM uranyl acetate was added last using a purged needle and syringe. All bacterial experiments were incubated at 30°C with gyratory shaking at 100 rpm for 7 to 14 days, while cells were metabolically active. Experiments with synthetic metaschoepite were conducted in PIPES buffer, pH 7. As the 10 mM metaschoepite stock was maintained in 30 mM PIPES, only 4 mL of 60 mM PIPES was added to tubes that received 1 mL of 10 mM metaschoepite.

2.3. Abiotic Experiments with AH_2DS and Fe(II)

For abiotic U(VI) reduction experiments, AH_2DS was produced via bacterially catalyzed reduction of AQDS by incubating *S. putrefaciens* CN32 with H_2 as the electron donor in the appropriate buffer. Quantitative reduction was typically achieved within 24 h. After AQDS was reduced, as measured by absorbance at 405 nm (Fredrickson et al., 1998), cells were removed by filtration (0.2 μm) in an O_2-free glovebag, the solution was purged, and uranyl acetate added to achieve the desired final concentration. Solutions were equilibrated at room temperature in pressure tubes sealed with thick butyl rubber stoppers.

Fe(II) goethite slurries were prepared by adding 0.9 g of the synthetic goethite to 20 mL of 60 mM PIPES, pH 7. The pH was adjusted to ~8 with 10 N NaOH. The slurry was sonicated for 1 h and then purged with N_2. The slurry was equilibrated in an anaerobic glovebag. After 24 h, 4.5 mL of a 20 mM, $FeCl_2$ solution was added to the slurry, followed by 15.5 mL of O_2-free deionized water. The pH of this suspension was 7.5. The Fe(II) was equilibrated with the goethite overnight. Two mL of this slurry was added to the pressure tubes to obtain a final Fe(II) concentration of 0.45 mM and final goethite

concentration of 50 mM. The concentration of dissolved Fe(II) after equilibration was 20.3 ($\pm$7) μM. The total Fe(II) concentration in this suspension, as determined by extraction with 0.5 N HCl, was 384 ($\pm$14) μM. After correcting for controls and $Fe(II)_{(aq)}$, the sorbed Fe(II) was determined to be 61.5 μmol/g (1.18 μmol/m^2) goethite. Suspensions of goethite with sorbed Fe(II) were equilibrated with uranyl acetate as described above for AH_2DS. For consistency with biotic experiments, abiotic experiments were also equilibrated for 7 to 14 days.

2.4. Analyses

At select timepoints, replicate tubes were transferred to an anaerobic (Ar:H_2, 95:5) glovebag (Coy Laboratory Products, Ann Arbor, MI, USA) and 1 mL of suspension was sampled with a syringe and filtered through a 0.2 μm polycarbonate or a 10 K mol. wt. cutoff (Pall Filtron, Northborough, MA, USA) filter. This fraction was considered the soluble fraction and analyzed for U(VI), where appropriate. To analyze for solids-associated U(VI), suspensions were extracted with either 100 mM $NaHCO_3$, pH 8.4 (Phillips et al., 1995a), or 0.5 mol/L $(NH_4)_2CO_3$, pH 9 (Duff et al., 1997a,b). The pH was measured under anaerobic conditions by using a Ross combination electrode. HCl-extractable Fe(II) was obtained by adding 1 mL of suspension to 1 mL of 1 N Ultrex HCl, mixing, and allowed to stand for at least 1 h before analyzing for Fe(II). This extraction is termed 0.5 N HCl, and has been shown to be an effective extractant of total Fe(II) from microbially reduced suspensions of crystalline Fe oxides (Zachara et al., 1998).

Fe(II) in acidified filtrates (0.2 μm) or extracts was determined by using the ferrozine assay (Stookey, 1970). Uranium was analyzed by using a kinetic phosphorescence analyzer (Brina and Miller, 1992) (KPA-10, Chemchek, Richland, WA, USA), specific for U(VI). Lactate concentrations were determined using an enzymatic assay (Sigma, St. Louis, MO, USA).

2.5. X-ray Diffraction

Settled mineral residue from the reduction experiments was removed from the pressure tubes to minimize liquid transfer and dried under anaerobic conditions; the dried solid was smeared on a glass slide for X-ray diffraction analysis. Slides were kept under an anoxic atmosphere until analysis. The X-ray diffraction (XRD) apparatus consisted of two Philips wide-range vertical goniometers with incident-beam 2-θ compensating slits, soller slits, fixed 2-mm receiving slits, diffracted beam graphite monochromators, and scintillation counter detectors. The X-ray source was a Philips XRG3100 X-ray generator operating a fixed-anode, long-fine-focus Cu tube at 45 Kv, 40 mA (1800 W). Instrument control was by means of Databox NIMBIM modules (Materials Data, Livermore, CA, USA).

2.6. Uranium X-ray Absorption Near Edge Structure Spectroscopy

The suspensions, in triplicate, were analyzed for U oxidation state in the solid phase directly using the X-ray microprobe beamline X26A at the National Synchrotron Light Source (NSLS; Brookhaven National Lab., Upton, NY, USA). Samples were prepared for XANES analyses by placing a small amount of solid material in a ~2 mm well in a Lucite plate and sealing with thick Kapton tape. Plates were then placed in canning jars and shipped to NSLS. Microfocusing optics were used to obtain a small X-ray beam. A double elliptical Au- or Rh-coated Kirkpatrick–Baez mirror system operated at a pitch of 2 mrad was used to focus a 350 μm^2 monochromatic beam at the U L_{III} absorption edge (17166 eV) down to a 15 $\times$ 20 μm^2 beam, resulting in a total flux of ~10^{10} photons/s (Eng et al., 1995; Smith and Rivers, 1995; Yang et al., 1995). A Si(Li) energy dispersive detector with an area of 30 mm^2, was mounted at 90° to the beam. The detector was positioned 2 to 3 cm from the sample and used to monitor and collect U Lα fluorescence X-rays. Collection time was determined with a monochromator tuned 10 eV above the U L_{III} absorption edge and the count rate was observed with the Si(Li) detector. The count rate was 50 counts/s for the U L_{III} edge. This was used to calculate the count time per scan point, which gave a scan maximum of >6000 counts. Three to eight seconds per scan point provided adequate counts for the 15 $\times$ 20 μm^2 X-ray beam size. XANES spectra were acquired at 0.3 to 2.5 eV step intervals over a 130 eV range, which was relative to 17166 eV. Scan limits were 40 eV less than and 90 eV greater than the U L_{III} absorption edge. Standards consisted of $U(IV)O_{2(s)}$, metaschoepite and U(VI)-acetate. The U L_{III}-XANES edge energies were defined as the height of the edge step. Edge energy values were calibrated to be 0 eV with a $UO_{2(s)}$ standard and monitored with $UO_{2(s)}$ before and after each sample. An increase with respect to the relative XANES energy edge indicates an increase in the average U oxidation state. A linear relationship has been shown between the fraction of U(VI) in the solid and relative XANES energy edge (Bertsch et al., 1994). The spectra were smoothed with the Savitsky–Golay method (Savitzky and Golay, 1964). Error in the XANES measurements is $\pm$10%. One sample from each triplicate was analyzed by XANES; the standard deviations reported reflect this error only.

2.7. Thermodynamic Calculations

Effective redox potentials (E′) were calculated for the various electron transfer reactions directly or indirectly mediated by *S. putrefaciens* by using the Nernst equation:

$$aA + bOx + ne^- = cC + dRed \quad (1)$$

$$E' = E° - RT/nF(\ln[\{C\}^c\{Red\}^d]/[\{A\}^a\{Ox\}^b] \quad (2)$$

where E° is the standard-state half-cell potential; {Ox} and {Red} are thermodynamic activities for oxidized and reduced species; {A} and {C} are thermodynamic activities for other reaction components (e.g., H^+, HCO_3^-, etc.); and R, T, and F are the gas constant, degrees Kelvin, and the Faraday constant, respectively. Thermodynamic activities for aqueous species were calculated by using MINTEQA2 (Allison et al., 1991) with the best available thermodynamic data compiled by the authors. Half-cell potentials, complexation constants, and solubility products for U(IV) and U(VI) species were primarily from Grenthe et al. (1992b and 1995), while those for the Fe(II, III) system were from Cornell and Schwertmann (1996); Bruno et al. (1992); and Langmuir (1997). The half-cell potential (E°) for the lactate to acetate biodegradation reaction was derived from data presented by Morel (1983).

3. RESULT

3.1. Bacterial Reduction of Uranyl Acetate in $NaHCO_3$ and PIPES Buffers

S. putrefaciens CN32 quantitatively reduced 100 μM uranyl acetate, with lactate or H_2 as an electron donor (data not shown), confirming previous results (Lovley et al., 1991). In both PIPES- and $NaHCO_3$-buffered suspensions, the decrease in $U(VI)_{aq}$ in CN32 cell suspensions with electron donor (Table 1) was accompanied by the formation of a dark gray to black precipitate that formed flocs with the bacterial cells. XANES spectra of the microbially reduced U(VI) flocs revealed a characteristic shift of the relative L_{III} edge energy (Fig. 1) indicative of U(IV) (Bertsch et al., 1994). The same treatments, but with heat-killed cells or microbially reduced U exposed to air for 12 h, had edge energies consistent with a predominant U(VI) oxidation state. The X-ray diffractogram of reduced flocs (Fig. 2), although exhibiting a relatively high signal-to-noise ratio and broad diffraction maxima, was consistent with the *d*-spacings for uraninite [$UO_{2(s)}$]. Uraninite was previously shown to be a product of uranyl acetate reduction by the dissimilatory iron-reducing bacterium *Geobacter metallireducens*, strain GS-15 (Gorby and Lovley, 1992). The broad diffraction maxima were indicative of the fine-grained character of the biogenic precipitate.

Table 1. Electron transfer to Fe(III) and U(VI) during lactate respiration by *S. putrefaciens* CN32.

Composition	Fe(II) μM	U(IV)[a] μm	U(VI)->U(IV) + Fe(III)->Fe(II) electrons, μM	Lactate consumed, mM	Lactate/Fe + U ratio
Schoepite, CN32, goethite, 1 mM lactate	2530	340	3200	bd[b]	3.2
Schoepite, CN32, goethite, 10 mM lactate	2690	860	4410	4.0	1.1
Schoepite, goethite, 1 mM lactate	280	bd[b]	280	nd[d]	—
Schoepite, CN32, goethite	210	bd[b]	210	nd[d]	—
Schoepite, CN32, 1 mM lactate	na[c]	830	1660	nd[d]	—
Schoepite, 1 mM lactate	na[c]	bd[b]	na[c]	nd[d]	—

[a] Estimated from U XANES.
[b] bd = below detection.
[c] na = not applicable.
[d] nd = not done.

3.2. Reduction of Uranyl Acetate in Goethite Suspensions

In suspensions containing 4.5 g/L goethite, *S. putrefaciens* CN32 also promoted the reduction of 1 mM uranyl acetate to an insoluble form in $NaHCO_3$-buffered solution with or without 100 μM AQDS (Fig. 3). U XANES revealed that U in the microbially reduced solids was predominantly U(IV), whereas in the unreduced controls it was essentially all U(VI) (e.g., 97%, Fig. 3).

In these experiments, AQDS was included as a model humic acid that contains a microbially reducible quinone (Lovley et al., 1996; Scott et al., 1998). AQDS has been shown to enhance the rate and extent of microbial reduction of solid Fe(III) oxides including goethite, hematite and natural crystalline Fe(III) oxides (Zachara et al., 1998). The presence of AQDS resulted in a smaller fraction of U(IV) in the solids (76 to 84%) than in its absence (97 to 100%), as determined by U XANES analyses (Fig. 3), even though the concentration of $U(VI)_{aq}$ was only slightly above detection in the $NaHCO_3$-buffered solution.

In suspensions with 1 mM lactate and CN32 cells, approximately 10% (5 mM) of the initial goethite was reduced (Fig. 4). In suspensions with 100 μM AQDS, the concentration of HCl-extractable Fe(II) was slightly higher, probably due to facilitation of electron transfer from the cells to the oxide surface (Zachara et al., 1998). Neither U nor Fe solid reduction products were evident upon examination of CN32-reduced U and goethite suspensions by scanning electron microscopy (SEM, data not shown). Solid phase reduction products such as siderite or uraninite were not apparent and diffraction maxima for either of these phases were not detected by XRD analysis (not shown). Siderite crystallites from CN32 reduction of Fe(III) oxides are typically 1 to 5 μm in size (Fredrickson et al., 1998; Zachara et al., 1998) and hence would have been evident in the SEM analyses. Uraninite formed by microbial reduction of U(VI) is fine-grained (Gorby and Lovley, 1992) and could be masked by the goethite.

The extent of Fe(III) reduction, and possibly U in the suspensions with AQDS was likely limited by available electron donor, 1 mM lactate. The number of moles of electrons from lactate used to reduce Fe and U by CN32 with or without of AQDS, were higher (29 to 58%) than the values that would be predicted from the oxidation of 1 mM lactate to acetate and CO_2. This suggests that lactate was completely consumed by CN32. This higher number of moles of electrons may be due to endogenous reserves of energy associated with the fresh cell cultures.

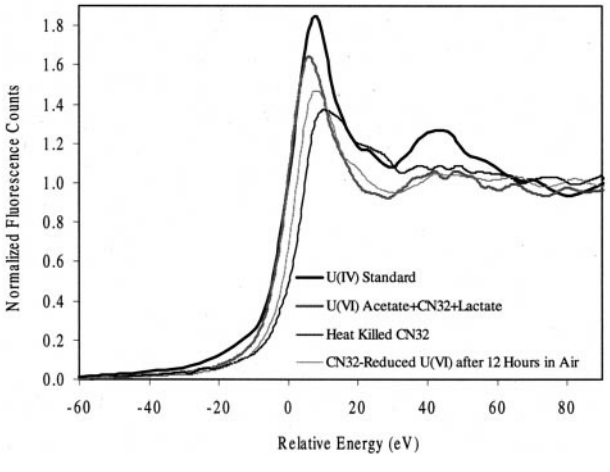

Fig. 1. Microprobe X-ray absorption near-edge structure (XANES) spectra of U in microbially reduced suspensions in $NaHCO_3$ buffer compared to a synthetic uraninite [$UO_{2(s)}$] standard, microbially reduced U after 24 h of exposure to air, and of U(VI) in heat-killed cell suspensions.

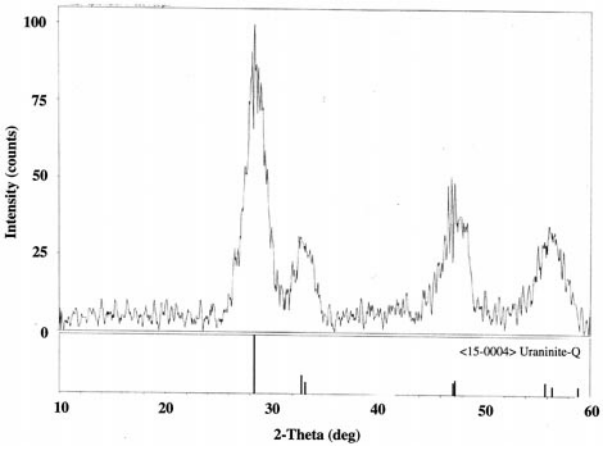

Fig. 2. X-ray diffractogram of solids produced upon microbial reduction of U(VI) acetate.

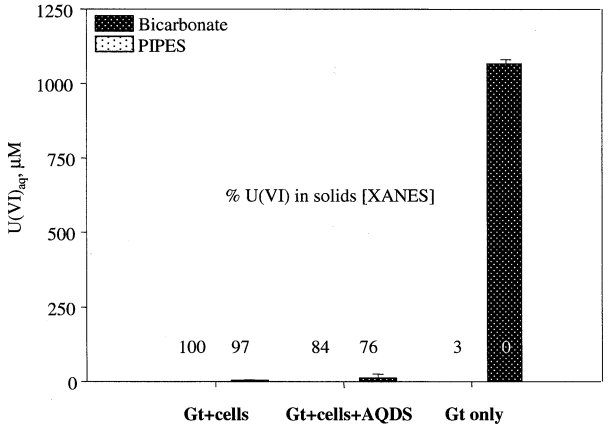

Fig. 3. Reduction of U(VI) acetate by *S. putrefaciens* CN32 in $NaHCO_3$ or PIPES buffered suspensions of 50 mM α-$FeOOH_{(s)}$ (Gt) with 1 mM lactate.

In solutions buffered with 30 mM $NaHCO_3$, pH 7, U(VI) was computed to be present primarily as the carbonate complexes $UO_2(CO_3)^{4-}_{3(aq)}$ and $UO_2(CO_3)^{2-}_{2(aq)}$. In comparison, 1 mM uranyl acetate in PIPES buffer, pH 7, exceeded the solubility of metaschoepite indicating potential for precipitation. The aqueous concentration of U(VI) in equilibrium with metaschoepite under these experimental conditions in PIPES buffer (as determined by calculation) is approximately $10^{-6.5}$ M. Uranyl acetate, at concentrations from 50 to 1800 μM, was equilibrated for 14 days in 30 mM, PIPES, pH 7, or $NaHCO_3$ buffers and the aqueous (0.001-μm filtered) U(VI) was measured. The concentration of $U(VI)_{aq}$ after equilibration in the $NaHCO_3$ buffer was unchanged (Fig. 5a), and in the PIPES buffer was less than 125 μM after equilibration regardless of initial U(VI) concentration (Fig. 5a). The computed $U(VI)_{aq}$ equilibrium speciation in the PIPES buffer was dominated by the hydroxo complexes $UO_2OH^+_{(aq)}$ or $UO_2(OH)^o_{2(aq)}$. These results indicate that in the previously described experiments in PIPES buffer, Figs. 1–3, most of the initial U(VI) concentration was present as a solid, possibly metaschopeite, and hence, the

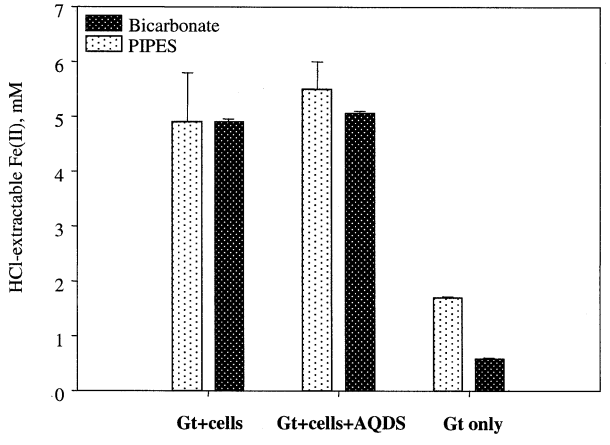

Fig. 4. Reduction of $FeOOH_{(s)}$ (Gt) by *S. putrefaciens* CN32, as measured by 0.5 N HCl-extractable Fe(II), in $NaHCO_3$ or PIPES buffered suspensions of 1 mM uranyl acetate with 1 mM lactate.

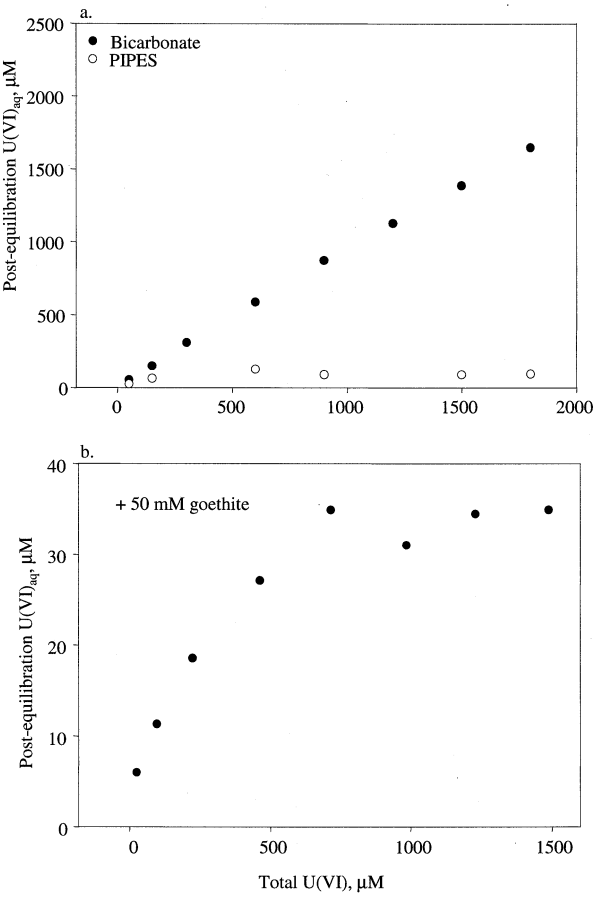

Fig. 5. Solubility of U(VI) acetate in suspensions in 30 mM $NaHCO_3$ or PIPES buffer after equilibration for 14 days (a) and sorption isotherm of U(VI) acetate to 50 mM $FeOOH_{(s)}$ in 30 mM $NaHCO_3$ buffer (b).

phase that the bacteria would have reduced. In equilibrated suspensions with 50 mM goethite, between 2 and 19%, depending on the initial U(VI) concentration, of the $U(VI)_T$ was sorbed to the goethite in the $NaHCO_3$ buffer (Fig. 5b). Due to the potential precipitation of metaschoepite in the PIPES-buffered goethite suspensions, it was not possible to determine with precision the amount of total U(VI) that may have been sorbed to goethite.

3.3. Influence of Goethite on the Bacterial Reduction of Metaschoepite

To further investigate the microbial reduction of solid-phase U(VI), the reduction of synthetic metaschoepite by CN32 in PIPES-buffered suspensions with and without goethite was examined. Without goethite, U(VI) extracted by 100 mM, pH 8.4 $NaHCO_3$ was less than 10% of the initial metaschoepite concentration in the suspension with CN32 and lactate. In the absence of cells, 94% of the initial U(VI) was recovered by this extraction procedure (Fig. 6). The decrease in bicarbonate-extractable U(VI) was attributed to bacterial reduction of metaschoepite to a U(IV) solid. Uranium XANES analyses of microbially reduced metaschoepite revealed a shift of the relative XANES energy edge to a lower energy edge (Fig. 7a)

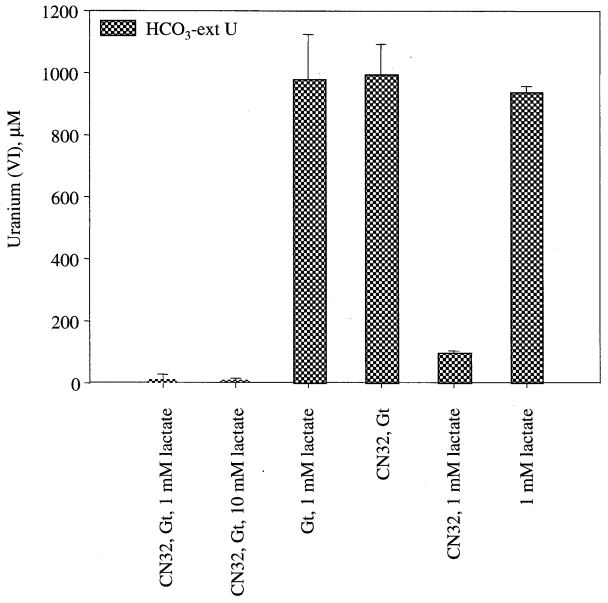

Fig. 6. Concentration of aqueous and 100 mM, pH 8.4 Na bicarbonate extractable U(VI) of bioreduced 1 mM metaschoepite [$UO_3 \cdot 2H_2O_{(s)}$] in suspensions with and without 50 mM $FeOOH_{(s)}$ (Gt).

indicative of tetravalent U. Based on this relative edge energy, 74 ± 10% of solid was U(IV).

In the metaschoepite suspensions with goethite, <1% of the initial U(VI) was recovered in the bicarbonate extractions of suspensions with 1 or 10 mM lactate, whereas >98% was recovered in the controls that lacked electron donor (lactate) or cells (Fig. 6). In contrast to metaschoepite suspensions without goethite, the relative XANES edge energy of the microbially reduced materials was shifted less in the presence of goethite and 1 mM lactate (Fig. 7b), and only 22 to 38% of the U in the solids was U(IV). In spite of this modest reduction of U(VI) from metaschoepite, remaining U(VI) was recalcitrant to extraction by Na bicarbonate, pH 8.4, or $(NH_4)_2CO_3$, pH 9. When lactate was increased to 10 mM, a greater proportion (86 ± 4%) of the U associated with the solids was U(IV), as determined by U XANES. TEM analyses of bioreduced goethite–metaschoepite suspensions revealed acicular goethite particles of approximately 0.2 μm in length (Fig. 8a) and the absence of obvious solid phase reduction products such as uraninite or siderite. Energy filter imaging, selective for uranium, in concert with TEM revealed very fine grained U particles, <10 nm in diameter, associated in patches with the goethite surfaces (Fig. 8b).

In the metaschoepite–goethite suspensions with CN32 cells and 1 mM lactate, the 2.5 mM Fe(II) extracted by 0.5 N HCl, when combined with the reduced U, accounted for 80% of the possible electrons from lactate respiration (Table 1) (Lovley, 1991). Lactate remaining after microbial reduction had ceased was below the detection limit indicating that the microorganisms had consumed all of it. The ratio of U(VI) + Fe(III) reduced (total electrons) to lactate consumed was 3.2, a value close to the theoretical stoichiometry. In contrast, only 4 mM was consumed in the identical experiment where 10 mM lactate was added and the ratio of U(VI) + Fe(III) reduced to lactate

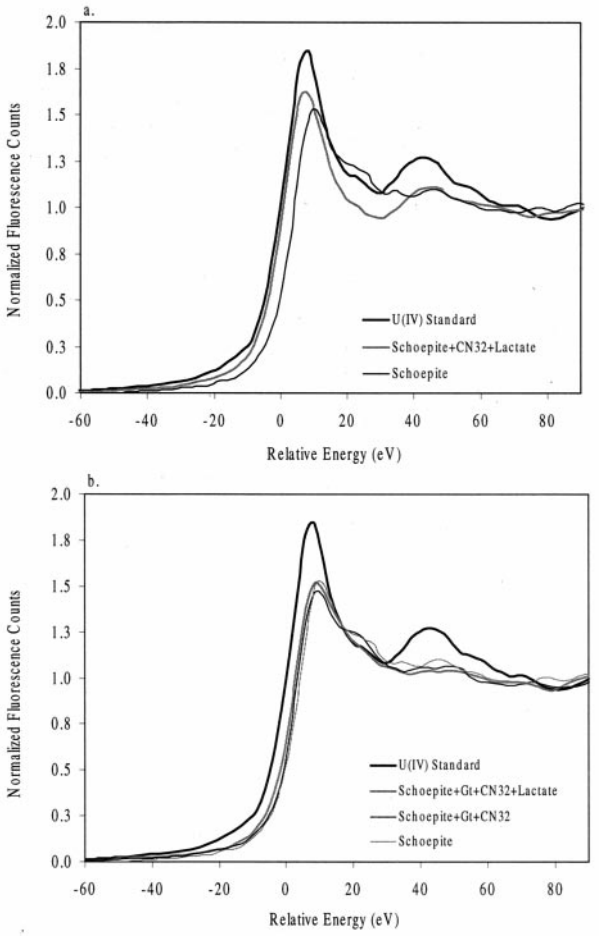

Fig. 7. Uranium XANES of microbially reduced metaschoepite with 1 mM lactate in the absence of $FeOOH_{(s)}$ (a) or in suspensions containing 4.4 g/L $FeOOH_{(s)}$ (b) in $NaHCO_3$ buffer in reference to a synthetic uraninite [$UO_{2(s)}$] standard, a control without electron donor (lactate), and unreduced metaschoepite.

consumed was 1:1. This indicates that factors other than electron donor limitation were responsible for cessation of Fe(III) and U(VI) reduction by CN32 in suspensions with 10 mM lactate.

The comparative bioreduction of U(VI) in PIPES-buffered goethite suspensions was intriguing. Two types of experiments were performed, one in which 1mM U(VI) was added as dissolved U(VI)-acetate and second where 1mM U(VI) was added as metaschoepite. Our synthetic preparation yielded XRD maxima consistent with the *d*-spacings for metaschoepite as reported by a number of investigators (e.g., Sowder et al., 1996). It was relatively fine-grained (~100 nm) and generally platy or tabular in morphology when viewed by HRTEM (Fig. 9a,b). The metaschoepite-spiked goethite suspension (second experiment) was considered to be a model of the phase in the first experiment. It was therefore unexpected when the bioreducibility of U(VI) was 97% in the U(VI) acetate-spiked (Fig. 3) compared to 22 to 38% in the metaschoepite-spiked goethite suspensions and 75% in the metaschoepite alone (Fig. 6). This sizable difference implied that chemical nature of the sorbed or precipitated U(VI) was different in the two experiments.

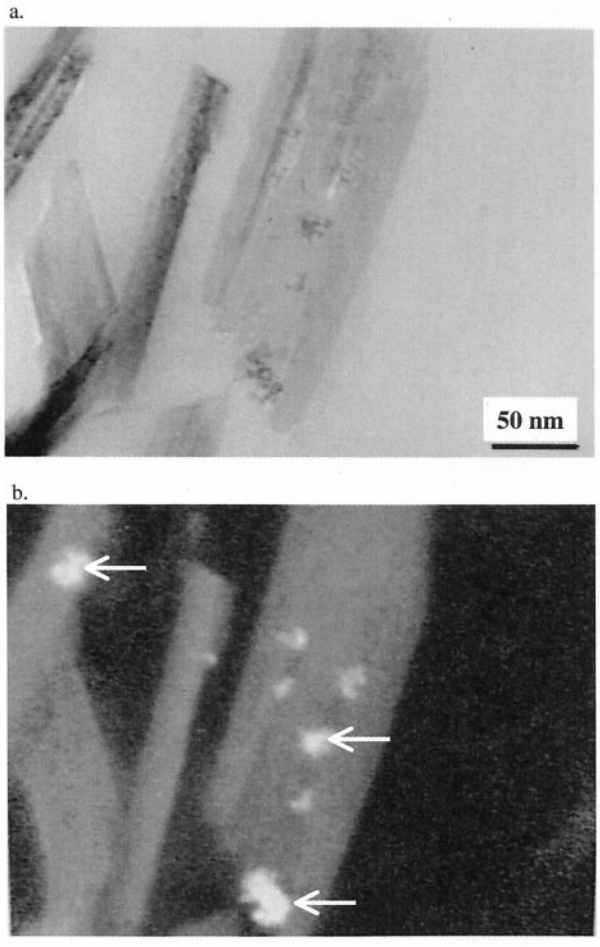

Fig. 8. TEM image of $FeOOH_{(s)}$ particles from bioreduced goethite–metaschoepite suspensions (a) and energy filtered TEM showing the U ratio image of the same field as in (b), revealing the localization of U (arrows) in association with goethite (b).

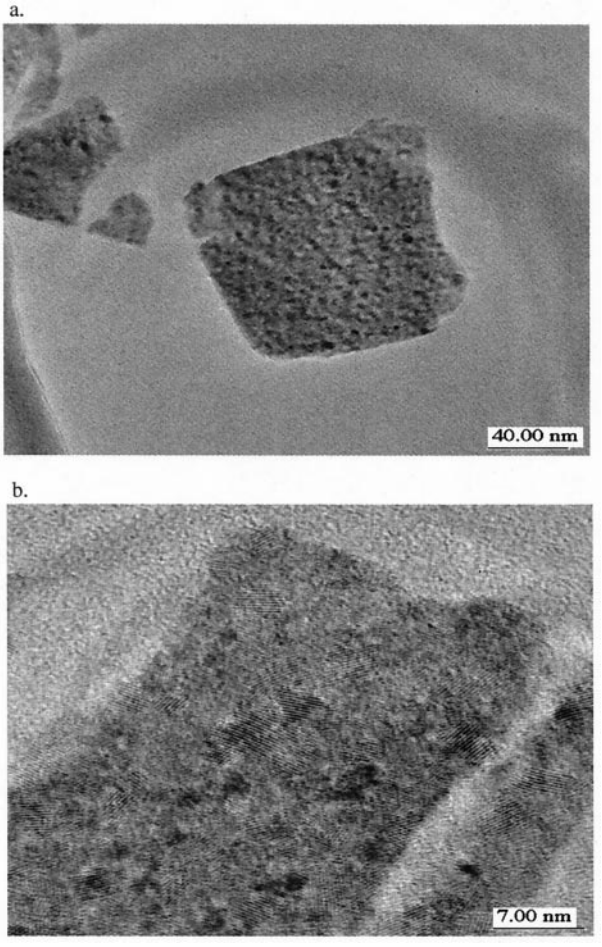

Fig. 9. Low magnification TEM image of a particle of the synthetic metaschoepite (a) and high magnification image illustrating the crystalline nature of the solid (b).

3.4. Abiotic Interactions of U(VI) with AH_2DS, $Fe(II)_{aq}$, and Sorbed Fe(II)

In suspensions containing goethite, AQDS, and U(VI), *S. putrefaciens* CN32 may be reducing all electron acceptors: 1) simultaneously [U(VI), Fe(III), and AQDS], or 2) preferentially due to differences in solubility, bioavailability, or more favorable energetics or kinetic pathways. Because of potential for electron acceptors to be utilized preferentially, the ability of AH_2DS and reduced Fe species (aqueous and sorbed) to reduce U(VI) was investigated. AQDS was quantitatively reduced to AH_2DS by CN32, filtered to remove cells and added, at a range of concentrations, to 1 mM uranyl acetate in 30 mM $NaHCO_3$ buffer, pH 7. The difference between the initial U(VI) concentration and the U(VI) extracted with 100 mM Na bicarbonate, pH 8.4, after equilibration was approximately equivalent to the starting AH_2DS concentration (Fig. 10). This indicates a quantitative reduction of aqueous U(VI) carbonate species by microbially reduced AQDS. Though the equilibration period for this experiment was 14 days, formation of a gray to black precipitate was noted within minutes after mixing the AH_2DS and U(VI). Metaschoepite, at 1 mM in 30 mM, PIPES buffer, pH 7, was also reduced by 200, 500, and 800 μM AH_2DS (data not shown). Analogous to the data in Fig. 7, the U XANES analysis of solids from experiments with metaschoepite revealed between 23 and 100% of the U associated with the solids was U(IV).

In contrast to AH_2DS, 2 mM $Fe(II)_{aq}$ was a less effective reductant of uranyl acetate in $NaHCO_3$ buffer, as all of the U(VI) and Fe(II) was recovered in the aqueous phase (Table 2). The XANES analyses indicated that some U(VI) ($\sim$18 $\pm$ 9%) was reduced by Fe(II) in the PIPES buffer (Table 2); consistent with this result was that a small fraction, 140 μM, of the initial $\sim$2 mM Fe(II) that was added was not recovered after equilibration (data not shown). When Fe(II) was preadsorbed to the surface of goethite and equilibrated with uranyl acetate in PIPES buffer [$Fe(II)_T$ = 384 $\pm$ 13 μmol/L; 61.5 μmol Fe(II)/g goethite], approximately 93, 72, and 20% of the U(VI) acetate at initial concentrations of 46, 93, and 460 μM, respectively was not extractable with 100 mM, $NaHCO_3$, pH 8.5 (Table 2). U XANES analyses of solids from the 460 μM U indicated that approximately 24% was U(IV), a value close to the 20% U not extractable with $(NH_4)_2CO_3$. Based on Fe(II) sorption iso-

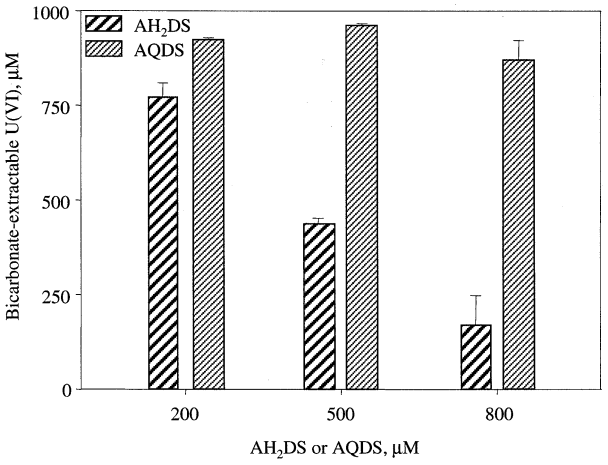

Fig. 10. Concentration of U(VI), initially present as U(VI) acetate in $NaHCO_3$ buffer, extracted with 100 mM, $NaHCO_3$, pH 8.4, after equilibration with microbially reduced AQDS (AH_2DS) or unreduced AQDS for 14 days.

therms conducted in 10 mM PIPES, pH 7, with this same goethite, the Fe(II) sorbed to goethite (1.18 μmol/m^2) was at approximately 37% of the maximum saturation (3.23 μmol/m^2; Zachara et al. 2000).

4. DISCUSSION

4.1. Conceptual Models of Bioreduction

The thermodynamic system investigated is one where electrons, from lactate, are mobilized during microbial respiration and, ultimately, transferred from the terminal point of the bacterial electron transport system to extracellular electron acceptors. In these studies, U(VI), FeOOH, and AQDS are potential acceptors. Their redox potentials as calculated for the specific experimental conditions are summarized in Table 3. The computations assumed pH 7 for the predominant aqueous [e.g., $Fe^{2+}_{(aq)}$, $UO_2(OH)^o_{2(aq)}$, etc.] and solid species [$FeOOH_{(s)}$, $UO_3 \cdot 2H_2O_{(s)}$, $UO_{2(s)}$] that were known or computed to be present. For example, the oxidation/reduction reaction for ferrous iron (Fe^{2+}, Reaction 4) was written with $Fe(OH)_{3(s)}$ as the oxidized species because it, rather than $Fe(OH)_2$ + or $Fe(OH)^o_3$ is the initial Fe^{2+}(aq) oxidation product (e.g., Eary and Rai, 1988). Lactate (Reaction 7) was the strongest reductant as indicated by E′, while $UO_2(OH)^o_{2(aq)}$ (Reaction 1) was the strongest oxidant. Complexation of $UO^{2+}_{2(aq)}$ by CO^{2-}_3 decreases the oxidation potential of U(VI) (Reactions 2 and 3). The two Fe couples were more reducing than all those of U(VI) at the specific pH and component concentrations used for the computation.

The bioreduction experiments with CN32 may, conceptually, be viewed as electron titration experiments. Bacteria provide the mechanism to enzymatically liberate electrons as they metabolize lactate. Specific constraints to microbial electron transfer, such as the requirement for direct cell contact with solid phase electron acceptors (Arnold et al., 1988; Lovley and Phillips, 1988; Myers and Nealson, 1988) (e.g., $FeOOH_{(s)}$ and $UO_3 \cdot 2H_2O_{(s)}$), must be considered. Microbial consumption of lactate (Reaction 7, Table 3) decreases the functional pϵ of the transfer of electrons to oxidized electron acceptors. Without kinetic constraints (which often predominate), the most strongly oxidizing species [e.g., $UO_2(OH)^o_{2(aq)}$] are expected to be reduced first, followed by the second [e.g., $(UO_2)_2CO_3(OH)^{3-}_{(aq)}$], etc., based on potential free energy change (e.g., Scott and Morgan, 1990; Zehnder and Stumm, 1988). It may thus be speculated based on arguments of thermodynamic feasibility that as lactate is consumed according to Reaction 7, the remaining reactions in Table 3 would proceed in sequence, 1, 2, 3–6, with due consideration given to the concentration of reactive components. However, the exact reduction sequence that occurs will be dictated by kinetic factors and enzymatic pathways and may differ from that predicted on thermodynamic grounds. Electron transfer between respiring DMRB and the Fe(III) oxide surface, for example, appears to be a kinetically slow process, being limited by complex factors at the organism–oxide interface involving attachment and surface complexation.

Alternatively, the bacteria in these experiments can be viewed as generating a "constant bio-potential." In this second

Table 2. Reduction of U(VI) acetate by $Fe(II)_{(aq)}$ or Fe(II) sorbed to goethite.

Components	$U(VI)_{aq}$, μM	HCO_3-U(VI)[a], μM	Estimated amount of U(VI) reduction[b] %
2 mM $Fe(II)_{aq}$, HCO^-_3, 1 mM uranyl acetate	1091 (42)	—	nd[c]
2 mM $Fe(II)_{aq}$, PIPES, 1 mM uranyl acetate[e]	0.01	—	18 (9)[d]
Fe(II), $FeOOH_{(s)}$, PIPES, 46 μM uranyl acetate[e,f]	bd	2.9 (4.9)[d]	nd[g]
$FeOOH_{(s)}$, PIPES, 46 μM uranyl acetate[e]	bd	41.9 (1.9)[d]	nd[g]
Fe(II), $FeOOH_{(s)}$, PIPES, 93 μM uranyl acetate[e,f]	bd	24.6 (18.9)[d]	nd[g]
$FeOOH_{(s)}$, PIPES, 93 μM uranyl acetate[e]	bd	89.1 (3.8)[d]	nd[g]
Fe(II), $FeOOH_{(s)}$, PIPES, 460 μM uranyl acetate[e,f]	bd	380.7 (36.3)[d]	24 (8.7)[d]
$FeOOH_{(s)}$, PIPES, 460 μM uranyl acetate[e]	bd	473.3 (43.2)[d]	8 (1.2)[d]

[a] Extractable with 100 mM N bicarbonate, pH 8.5.
[b] As estimated from XANES L_{III} edge position, analysis requires solid materials.
[c] No solids formed in this solution.
[d] Standard deviation.
[e] Initial U concentration supersaturated with schoepite, precipitation expected and indicated by color change at the higher concentration.
[f] Total Fe(II) = 2.97×10^{-4} M, adsorbed (Fe(II) = 67.5 μmol Fe(II)/g goethite.
[g] U_T was too low for XANES analyses.

Table 3. Reduction potentials of chemical components.

Reaction	E°(v)	E′(v)	Comment
1) 0.5 $UO_2(OH)^{\circ}_{2\,(aq)}$ + H^+ + e^- = .5 $UO_{2(s)}$ + H_2O	0.757	0.139	Simulation of PIPES treatment $U_T = 1.0 \times 10^{-3}$ mol/L, saturated with schoepite giving $U_{T(aq)} = 2.7 \times 10^{-7}$ mol/L and $\{UO_2(OH)^{\circ}_{2\,(aq)}\}^b = 1.3 \times 10^{-7}$
2) 0.25 $(UO_2)_2CO_3(OH)^-_{3(aq)}$ + H^+ + e^- = 0.5 $UO_{2(s)}$ + 0.75 H_2O + 0.25 HCO_3^-	0.576	0.139	Simulation of PIPES bioreduction experiment, CO_3 from lactate metabolism. $U_{T(aq)} = 2.9 \times 10^{-5}$ mol/L fixed by schoepite solubility. $\{(UO_2)_2CO_3(OH)_3^-\} = 8.8 \times 10^{-6}$; $C_T = 5.0 \times 10^{-4}$ mol/L.
3) 0.5 $UO_2(CO_3)^{4-}_{3(aq)}$ + 1.5 H^+ + e^- = 0.5 $UO_{2(s)}$ + 1.5 HCO_3^-	0.687	0.078	Simulation of bicarbonate treatment, $U_T = U_{T(aq)} = 1.0 \times 10^{-3}$ mol/L unsaturated with schoepite. $\{UO_2(CO_3)_3^{4-}\}^b = 1.5 \times 10^{-5}$; $C_T = 3.05 \times 10^{-2}$ mol/L
4) $Fe(OH)_{3(s)}$(fresh) + 3H^+ + e^- = $Fe^{2+}_{(aq)}$ + 3H_2O	1.064	−0.018	$\{Fe^{2+} = 1.0 \times 10^{-3}\}^b$
5) $FeOOH_{(S)}$ + 3H^+ + e^- = $Fe^{2+}_{(aq)}$ + 2H_2O	0.799	−0.088	$\{Fe^{2+} = 1.0 \times 10^{-6}\}^b$
6) 0.5 AQDS + H^+ + e^- = 0.5 AH_2DS	0.230	−2.40	$\{AQDS\} = 1.0 \times 10^{-6}$; $\{AH_2DS\} = 1.0 \times 10^{-4}$
7) 0.125 CH_3COO^- + 0.25 HCO_3^- + 1.20 H^+ + e^- = 0.166/L[a] + 0.50 H_2O	0.121	−0.410	PIPES buffer, 10 mM initial lactate; 4.0 mM utilized during bioreduction (e.g., Table 1)
		−0.396	30 mM bicarbonate buffer, 10 mM initial lactate; 4.0 mM lactate utilized during bioreduction
		−0.436	PIPES buffer, 1 mM initial lactate, 0.1 mM lactate utilized
		−0.403	PIPES buffer, 1 mM initial lactate, 0.95 mM lactate utilized

[a] L = lactate.
[b] { } = activity.

model, a constant, low reductive potential develops on the microbe surface, in conjunction with electron transfer proteins in the outer membrane (Beliaev and Saffarini, 1998; Myers and Myers, 1997; Myers and Myers, 1998). The potential may vary for electron donors because of their chemical potentials, (e.g., lactate versus H_2), but is manifest in the effective redox potential of cytochromes or other electron transfer proteins at the organism surface. For lactate, this potential could range from between −440 and −400 mV (Table 3, Reaction 7). Midpoint potentials of *c*-type cytochromes from anaerobic bacteria as low as −400 mV have been measured (Bianco and Haladjian, 1994), although the lowest potential measured for a *c*3-type cytochrome in *S. putrefaciens* is −233 mV (Tsapin et al., 1996). Any electron acceptor that has a higher E′ than the values noted can potentially be reduced by the "constant potential" organism surface. The competition between, or preference for, electron acceptors may be explained by two factors: the species-specific enzyme mediated electron transfer kinetics; and mass transfer of the electron acceptor to the active site on the enzyme.

For solids, this situation is complicated by several factors including organism–surface contact area, spatial location and "mobility" of competing electron acceptor solids, their solubility, etc. With a "constant bio-potential" model, CN32 could reduce $FeOOH_{(s)}$ in presence of metaschoepite, in spite of the higher oxidation potential of the U(VI)-couple, because the cells are predominantly associated with goethite surfaces and develop a surface potential capable of reducing Fe(III) in goethite. The fact that metaschoepite is present in the system, some of which may also be in contact with cells, has no direct impact on Fe(III) reduction. Global equilibrium is achieved, if indeed such a point is reached at all, by abiotic electron transfer between kinetically viable redox couples that are in disequilibrium [e.g., Fe(II) in various states and U(VI)]. These abiotic reactions act to bring the redox potential of all other couples in balance with the organism surface.

4.2. Bioreduction of Uranium

4.2.1. Metaschoepite

This is the first report that we are aware of demonstrating the direct bacterial reduction of a crystalline U(VI) solid. *S. putrefaciens* has a remarkable ability to reduce solid phase metal oxides and oxyhydroxides with low metal solubility, including synthetic hydrous ferric oxide (HFO), goethite [α-$FeOOH_{(s)}$], hematite [α-$Fe_2O_{3(s)}$], magnetite [$Fe_3O_{4(s)}$], and crystalline Fe(III) oxides in subsurface sediments (Dong et al., 2000; Zachara et al., 1998). Although unknown, it is likely that the same mechanism that allows *S. putrefaciens* to reduce Fe(III) oxides and oxyhydroxides is responsible for their ability to reduce solid phase U(VI). Whether U(VI) is a soluble species or associated with a solid phase, *S. putrefaciens* can reduce it to insoluble $UO_{2(s)}$ in the absence of competing electron acceptors.

4.2.2. The impacts of goethite

Results of U bioreduction experiments are summarized in Table 4. Goethite did not impact the ability of *S. putrefaciens* CN32 to promote the reduction of U(VI), originally added as U(VI) acetate, in either $NaHCO_3$ or PIPES buffers. This was shown by a decrease in $U(VI)_{aq}$ in the $NaHCO_3$ buffer to below detection and the presence of predominantly U(IV) solids in both buffers, as determined by XANES (Fig. 3). In these suspensions, approximately 10% of the goethite was reduced (Fig. 4); this value is consistent with previous values (Zachara et al., 1998).

U(VI) sorbs strongly to Fe(III) oxide surfaces in the absence of CO_3^{2-} (Duff and Amrhein, 1996; Hsi and Langmuir, 1985; Waite et al., 1994), and it is plausible that the goethite surface modified the nature of the U(VI) precipitate from that of metaschoepite through a surface induced precipitation process. Perhaps the precipitate existed as microclusters on the goethite surface that allowed for optimal organism contact. The precip-

Table 4. Summary of uranium bioreduction experiments.

Components	Presumed U(VI) species/phase	Nominal % U(VI) reduction	Nominal % Fe(III) reduction
10 mM lactate (or 10 mL H_2), HCO_3^- buffer, 0.1 mM U_T as uranyl acetate	$UO_2(CO_3)^{4-}_{3(aq)}$, $UO_2(CO_3)^{2-}_{2(aq)}$[a]	>98	—
10 mM lactate (or 10 mL H_2); PIPES, 1 mM U_T as uranyl acetate	$UO_2OH^+_{(aq)}$ or $UO_2(OH)^0_{2(aq)}$,[a] unknown solid[b]	>98	—
1 mM lactate, 50 mM goethite, HCO_3^-, 1 mM U_T as uranyl acetate	$UO_2(CO_3)^{4-}_{3(aq)}$, $UO_2(CO_3)^{2-}_{2(aq)}$[a]	100	~10
1 mM lactate, 50 mM goethite, PIPES, 1 mM U_T as uranyl acetate	$UO_2OH^+_{(aq)}$ or $UO_2(OH)^0_{2(Aq)}$,[a] unknown solid[b]	97	~10
1 mM lactate, 50 mM goethite, 0.1 mM AQDS, HCO_3^-, 1 mM U_T as uranyl acetate	$UO_2(CO_3)^{4-}_{3(Aq)}$, $UO_2(CO_3)^{2-}_{2(aq)}$[a]	84	~10
1 mM lactate, 50 mM goethite, 0.1 mM AQDS, PIPES, 1 mM U_T as uranyl acetate	$UO_2OH^+_{(aq)}$ or $UO_2(OH)^0_{2(aq)}$,[a] unknown solid[b]	76	~10
1 mM lactate, PIPES, 1 mM U_T as $UO_3 \cdot H_sO_{(S)}$	Schoepite	83	—
1 mM lactate, 50 mM goethite, PIPES, 1 mM U_T as $UO_3 \cdot H_2O_{(S)}$	Schoepite	34	~5
10 mM lactate, 50 mM goethite, PIPES, 1 mM U_T as $UO_3 \cdot H_2O_{(s)}$	Schoepite	86	~5

[a] Predominant computed aqueous species.
[b] U(VI) may be present as a schoepite-like phase or an adsorbed species.

itate may have been amorphous and, because of the shorter aging time, exhibited higher solubility (e.g., Bruno and Sandino, 1989) and ease of reducibility by analogy to Fe(III) oxides (Roden and Zachara, 1996). The nominal hydroxyl surface site concentration of the goethite suspensions (4.4 g/L) was 0.88 mM [based on measurements by (Zachara et al., 2000) and other reports of goethite surface site density] and it is possible that 50% or more of the U(VI) spike (1 mM uranyl acetate) was adsorbed by goethite in the absence of $NaHCO_3$ buffer. Whether a surface precipitate, an adsorbed species, or a mixture, it is important to note that cells, lactate and uranyl acetate were added to the goethite suspension at the same time. Because U(VI) reduction is relatively rapid in the absence of goethite (0.45 μmol/min/L; Y. Gorby, unpublished data), it is possible that bacterial U(VI) reduction occurred concurrently with other geochemical reactions (e.g., precipitation).

Goethite did have a significant impact on the reduction of metaschoepite by CN32 with only 22 to 38% of the U(VI) being reduced compared to approximately 75% in its absence (Figs. 7a,b; Table 4). Due to its ability to form strong complexes with U(VI), bicarbonate has often been used to extract U(VI) from soils and sediments (Duff et al., 1997a,b; Phillips et al., 1995a). In our experiments, 100 mM, O_2-free, $NaHCO_3$, pH 8.4, or 0.5 mol/L, $(NH_4)_2CO_3$, pH 9, quantitatively extracted metaschoepite from abiotic controls with goethite, yet was ineffective at extracting residual U(VI) from reduced metaschoepite, especially in the presence of goethite (Fig. 6). There are several possible explanations for these observations. First, the effectiveness of the bicarbonate for extracting U(VI) in the presence of high concentrations of Fe(II) is unknown. After microbial reduction, bicarbonate may have complexed some of the Fe(II) and precipitated as siderite [$FeCO_{3(s)}$]. Precipitation of siderite and physical coating of metaschoepite could partially account for the ineffective extraction of U(VI) by bicarbonate.

Alternatively, microbial reduction of U(VI) may have lead to formation of a $UO_{2(s)}$ film or coating on the surface of metaschoepite, blocking subsequent reduction by the bacteria and extraction of U(VI) by bicarbonate. We are unaware of any reports of the formation of reduced U films on U(VI) solids, but thin oxidation films (UO_{2+x}), promoted by radiolysis products, have been observed on the surfaces of $UO_{2(s)}$ fuel (Hocking et al., 1992; Shoesmith et al., 1989) eventually resulting in metaschoepite covering the surface (Sunder et al., 1992). Air oxidation of UO_2 fuel at 200°C resulted in complete surface coverage by relatively large schoepite crystals that were subsequently replaced by small crystals of U_3O_8 (Taylor et al., 1991). Peterson et al. (1997) demonstrated that the surface of magnetite was passivated against further reaction with Cr(VI) by formation of a surface layer (10 to 20 Å) of maghemite after the initial reduction of Cr(VI) to Cr(III). In addition to formation of a $UO_{2(s)}$ film, it is also possible that amorphous $Fe(III)(OH)_{3(s)}$ (e.g., HFO) may have formed on the surface of the metaschoepite through reaction with biogenic Fe(II).

Formation of a $UO_{2(s)}$ or HFO film on the metaschoepite would also account for its incomplete reduction by *S. putrefaciens*. Lactate became limiting in metaschoepite–goethite suspensions at 1 mM. Differences in U(VI) reduction between 1 and 10 mM lactate treatments may have resulted because HFO, generated via oxidation of Fe(II) at the metaschoepite surface, did not accumulate with higher electron donor because lactate was not limiting (Table 1). The Fe(II) oxidized at the surface of the metaschoepite could have been reduced by the bacteria until lactate or other factors limited further bacterial reduction. We also evaluated another hypothesis that the increase in lactate concentration from 1 to 10 mM enhanced metaschoepite reduction by solubilizing U(VI) through aqueous complexation. Aqueous complexation constants (25°C, I = 0) for UO_2^{2+} with 2-hydroxy propanoic acid (lactate) were found to be log * $\beta_{1,1}$ = 3.16 and log * $\beta_{2,1}$ = 4.83 (Smith and Martell, 1995). Through multi-component speciation calculation (MINTEQA2), we observed that lactate competed poorly with hydroxide for UO_2^{2+} when the above constants were used. The 10-fold increase of lactate yielded a minimal change in the computed total aqueous UO_2^{2+} concentration, increasing it from 1.73 μM to 1.78 μM. At 10 mM lacatate, UO_2^{2+}-lactate complexes

represented <3% of $UO^{2+}_{2(aq)\text{-tot}}$, with the remainder being hydoxy complexes. It appears unlikely, therefore that aqueous complexation caused the noted enhancement in schoepite reduction as the lactate concentration was increased.

4.2.3. The influence of AQDS

We have shown previously that AQDS stimulates the rate and overall extent of dissimilatory Fe(III) reduction when the electron donor is not limiting, and influences the composition and crystallinity of biomineralization products (Fredrickson et al., 1998; Zachara et al., 1998). In suspensions of goethite in $NaHCO_3$ buffer, for example, siderite was noted as a biomineralization product of reduction by *S. putrefaciens* when AQDS was present but not in its absence. The mechanism by which AQDS stimulates bacterial Fe(III) oxide reduction has not been resolved but involves electron shuttling between the organisms and oxide, enhanced access to solid phase interstices and biologically inaccessible regions, and, possibly, modification of the bacterial microenvironment.

We expected that AQDS would stimulate both U(VI) and $FeOOH_{(s)}$ reduction based on previous results, and that AQDS would have greater effects on solid phase U(VI) reduction because fine-grained U(VI) precipitates (e.g., Fig. 9) and adsorbed species would be more accessible to a reduced solute of small dimension. In contrast, we observed that AQDS did not enhance $FeOOH_{(s)}$ reduction (Table 4), and its presence lowered the amount of U(VI) reduction compared to identical systems without it. This inhibitory effect on U(VI) reduction was small (e.g., approximately 10%), but discernible whether U(VI) was present as an aqueous or solid-associated species. One reason for the differences between these and past published experiments was the lactate concentration, which appeared to become limiting in the present experiments with 1 mM lactate. An explanation for the inhibitory effect of AQDS on U(VI) reduction was not apparent.

4.3. Abiotic Reactions

Alternate electron acceptors, such as $FeOOH_{(s)}$ and AQDS, were reduced with U(VI) during the microbial oxidation of lactate over incubation periods of 7 to 14 days, in qualitative agreement with a "constant bio-potential" model (see Section 4.1). Reduced products of these alternate reactions [e.g., $Fe^{2+}_{(aq)}$, sorbed Fe(II), and AH_2DS], in turn, exhibited thermodynamic potential to function as abiotic reductants of U(VI) (Table 3) and their kinetic ability to do so was evaluated in abiotic experiments (Table 2 and Fig. 10).

Microbially reduced AQDS was a facile reductant of U(VI), stoichiometrically reducing both aqueous [$UO_2(CO_3)^{4-}_{3(aq)}$, Reaction 3 in Table 3; Fig. 10] and solid phase U species [$UO_3 \cdot 2H_2O_{(s)}$, Reaction 1 in Table 3] to poorly crystalline uraninite. AH_2DS is a strong reductant (Table 3), with E′ considerably lower than that of the U(VI) couples (Table 3). The high reactivity of AH_2DS toward U(VI) in different coordination environments is quite remarkable. AQDS is readily reduced by DMRB (Fredrickson et al., 1998; Lovley et al., 1996), indicating ease of engagement with the DMRB electron transport chain.

Aqueous Fe(II) (2 mM) was ineffective as a reductant of U(VI) compared to AH_2DS (Table 2). The computed E′ of the iron couple [$Fe(OH)_{3(s)}/Fe^{2+}_{(aq)}$] indicated that $Fe^{2+}_{(aq)}$ should reduce U(VI) in both PIPES (Table 3, Reaction 1) and $NaHCO_3$ buffer (Table 3, Reaction 3) at pH 7, but the driving force for the latter reaction [with $UO_2(CO_3)^{4-}_{3(aq)}$] is small. The E′ of the Fe couple is strongly dependent on pH (e.g., $\pm$ 0.018 V/0.1 pH), thus consideration of the actual experimental pH is essential. Uranium remained fully soluble in the $NaHCO_3$ buffer [presumably as $UO_2(CO_3)^{4-}_{3(aq)}$] after equilibration with $Fe^{2+}_{(aq)}$ (Table 2), implying no reduction to U(IV). Reaction thermodynamics were marginally feasible at the measured pH (E′ values of 0.104 and 0.043 for Reactions 1 and 3, respectively, at pH 6.7). It is therefore unclear whether the lack of reduction resulted from kinetic or thermodynamic factors. The comparison of pertechnetate (TcO^-_4) and chromate (CrO^{2-}_4) is illustrative of the potential kinetic complexity. The reduction of both of these anions by $Fe(II)_{(aq)}$ is thermodynamically favorable, but only CrO^-_4 is appreciably reduced at circumneutral pH (Cui and Eriksen, 1996; Eary and Rai, 1988). The reduction inefficiency of $Fe(II)_{(aq)}$ in $NaHCO_3$ buffer did not result from its complexation (computed to be 27% by CO^{2-}_3) or mass loss through precipitation of siderite [$FeCO_{3(s)}$] as this phase was not observed although it may have been present at concentrations too low to detect by XRD.

Partial reduction of metaschoepite by $Fe^{2+}_{(aq)}$ occurred in PIPES buffer (8 to 18%, Table 2), consistent with the more favorable thermodynamics of the reaction 1/4 pair (Table 3). The heterogeneous reduction of $UO_3 \cdot 2H_2O_{(s)}$ by $Fe^{2+}_{(aq)}$ is a complicated kinetic process involving adsorption [of $Fe^{2+}_{(aq)}$] and surface precipitation [of $Fe(OH)_{3(s)}$, e.g., Bruno et al., 1995].

Fe(II) sorbed to goethite promoted greater reduction of precipitated U(VI) in PIPES buffer than did $Fe^{2+}_{(aq)}$, and extent of reduction was dependent upon the total U(VI) concentration (Table 2). The total Fe(II) in these suspensions (2.97×10^{-4} M) was intermediate in concentration to U(VI) (Table 2) and represented 67.5 μmol Fe(II)/g of goethite. Sorbed Fe(II) did not react to completion with U(VI), regardless of U(VI)/Fe(II) ratio. The thermodynamic feasibility of this reaction is not known. Stumm cites an E^o_H for the Fe(II)/Fe(III) surface complex couple of 0.36V (Stumm, 1992). This E^o_H, is relatively oxidizing and would not lead to the reduction of U(VI) (Table 3). However, Liger at al. (1999) recently reported the reduction of U(VI) by the Fe(II) complexes, $\equiv FeOFe^+$ and $\equiv FeOFeOH^0$, on the surface of hematite. The hydroxo complex $\equiv FeOFeOH^0$ was the rate determining reductant species and the initial rate of U(VI) reduction exhibited a first-order behavior with respect to sorbed uranyl concentration. Empirical evidence suggests that sorbed Fe(II) on goethite is a powerful and kinetically facile reductant (Cui and Eriksen, 1996; Haderlein and Pecher, 1999; Klausen et al., 1995; Rugge et al., 1998) which is consistent with our results. The presence of separate solid-phase reactants may impose severe mass transfer limitations on this reaction in our study, limiting the frequency of reactant contact and their effective concentrations.

5. IMPLICATIONS TO IN SITU U BIOIMMOBILIZATION

S. putrefaciens strain CN32, isolated from a U-enriched sandstone, effectively coupled the oxidation of lactate to the

reduction of U(VI) initially present as either a soluble carbonate complex or as a solid (metaschoepite) or adsorbed phase. Goethite functioned as a competing acceptor for electrons from lactate respiration and was partially reduced. It did not, however, impede the reduction of aqueous U(VI) to insoluble U(IV). Our experiments with U(VI) and $FeOOH_{(s)}$ do not allow differentiation of enzymatic versus non-enzymatic U(VI) reduction. U(VI) and Fe(III) were reduced concurrently where high cell densities and large electron donor concentrations were used to accelerate the bioreduction process. Measurements were not performed to assess the relative reduction rates of these two electron acceptors as this issue was beyond the scope of the current research. What is certain is that reduction of $FeOOH_{(s)}$ occurred enzymatically by *S. putrefaciens* as the Fe(III) oxide is not vulnerable to reduction by U(VI) for reasons of both solubility and thermodynamics. In contrast, goethite prevented the quantitative reduction of metaschoepite and altered the extractability of residual U(VI) in metaschoepite by bicarbonate. Metal-reducing bacteria can also potentially reduce U(VI) indirectly via the reduction of humic acids (e.g., AQDS) and Fe(III). This combination of direct and indirect microbial reduction can effectively immobilize U(VI) in the presence of Fe(III) oxides. Such a process may be feasible in situ, for immobilizing U in initially oxidizing subsurface environments.

Although synthetic goethite was used herein, previous research has shown that naturally occurring Fe(III) oxides are equally or more susceptible to microbial reduction (Zachara et al., 1998). Those findings, coupled with the potential for indirect reduction via microbial generation of Fe(II), suggests that metal-reducing bacteria would also promote U reduction and immobilization in Fe(III) oxide containing subsurface material. In subsurface environments, contaminant plumes of soluble U(VI) may be transported into anoxic zones where dissimilatory iron reduction is operative. Studies of ferrigenic groundwaters are limited but those performed generally indicate that: 1) the rates of bacterial reduction being both substrate and nutrient (e.g., P) limited are slow; and 2) aquifer surfaces are saturated with sorbed, biogenic Fe(II) from long term in situ enzymatic reduction of Fe(III) oxides (Heron et al., 1994a). Under these circumstances, the reduction of U(VI), if it occurs, may be dominated by reaction with biogenic Fe(II) products rather than directly by enzymatic activity.

Acknowledgments—This research was supported by the Natural and Accelerated Bioremediation Research Program (NABIR), Office of Biologic and Environmental Research, U.S. Department of Energy (DOE). Pacific Northwest National Laboratory is operated for the DOE by Battelle Memorial Institute Grant DE-AC06 to 76RLO 1830. Part of this research was supported by Financial Assistance Award No. DE-FC09 to 96R18546 from DOE to the University of Georgia Research Foundation. The X26A microprobe beamline is supported inpart by DOE Grant DE-FG02 to 92ER14244. We thank the NSLS staff for assistance. We also wish to thank Alice Dohnalkova for HRTEM, Paul Gassman for XRD analyses, David Boone (Portland State University) for providing *S. putrefaciens* CN32 to us from the Subsurface Microbial Culture Collection, and the insightful comments of three anonymous reviewers.

REFERENCES

Abdelouas A., Lu Y., Lutze W., and Nuttall H. E. (1998) Reduction of U(VI) to U(IV) by indigenous bacteria in contaminated groundwater. *J. Contam. Hydrol.* **35,** 217–233.

Allison J. D., Brown D. B., and Novo–Gradac K. J. (1991) MINTEQA2/PRODEFA2, A geochemical assessment model for environmental systems: Version 3.0 user's manual. U.S. Environmental Protection Agency.

Anderson R. F. (1987) Redox behavior of uranium in an anoxic marine basin. *Uranium* **3,** 145–164.

Arnold R. G., DeChristina T. J., and Hoffman M. R. (1988) Reductive dissolution of Fe(III) oxides by *Pseudomonas* sp. 200. *Biotechnol. Bioengineer.* **32,** 1081–1096.

Beliaev A. S. and Saffarini D. A. (1998) *Shewanella putrefaciens* mtrB encodes an outer membrane protein required for Fe(III) and Mn(IV) reduction. *J. Bacteriol.* **180,** 6292–6297.

Bertsch P. M., Hunter D. B., Sutton S. R., Bajt S., and Rivers M. L. (1994) In situ chemical speciation of uranium in soils and sediments by micro x-ray absorption spectroscopy. *Environ. Sci. Technol.* **28,** 980–984.

Bianco P. and Haladjian J. (1994) Recent progress in the electrochemistry of c-type cytochromes. *Biochimica* **76,** 605–613.

Boone D. R., Liu Y., Zhao Z. J., Balkwill D. L., Drake G. R., Stevens T. O., and Aldrich H. C. (1995) *Bacillus infernus* sp. nov., an Fe(III)- and Mn(IV)-reducing anaerobe from the deep terrestrial subsurface. *Int. J. Syst. Bacteriol.* **45,** 441–448.

Brina R. and Miller A. G. (1992) Direct detection of trace levels of uranium by laser-induced kinetic phosphorimetry. *Anal. Chem.* **64,** 1413–1418.

Bruno J. and Sandino A. (1989) The solubility of amorphous and crystalline schoepite in neutral to alkaline aqueous solutions. *Mat. Res. Soc. Symp. Proc.* **127,** 871–878.

Bruno J., Wersin P., and Stumm W. (1992) On the influence of carbonate in mineral dissolution: II. The solubility of $FeCO_{3(s)}$ at 25°C and I atm total pressure. *Geochim. Cosmochim. Acta* **56,** 1149–1155.

Casas I., De Pablo J., Gimenez J., Torrero M. E., Bruno J., Cera E., Finch R. J., and Ewing R. C. (1998) The role of pe, pH, and carbonate on the solubility of UO_2 and uraninite under nominally reducing conditions. *Geochim. Cosmochim. Acta* **62,** 2223–2231.

Cornell R. M. and Schwertmann U. (1996) *The Iron Oxides*. VCH.

Cui D. and Eriksen T. E. (1996) Reduction of pertechnetate by ferrous iron in solution: Influence of sorbed and precipitated Fe(II). *Environ. Sci. Technol.* **30,** 2259–2262.

Dong H., Fredrickson J. K., Kennedy D. W., Zachara J. M., and Onstott T. C. (2000). Mineral transformations associated with the microbial reduction of magnetite. *Chem. Geol.* (in press).

Duff M. C. and Amrhein C. (1996) Uranium(VI) adsorption on goethite and soil in carbonate solutions. *Soil Sci. Soc. Am. J.* **60,** 1393–1400.

Duff M. C., Amhrein C., Bertsch P., and Hunter D. B. (1997a) The chemistry of uranium in evaporation pond sediment in the San Joaquin Valley, California, USA, using X-ray fluorescence and XANES techniques. *Geochim. Cosmochim. Acta* **61,** 73–81.

Duff M. C., Amrhein C., and Bradford G. (1997b) Nature of uranium contamination in the agricultural drainage water evaporation ponds of the San Joaquin Valley, California, USA. *Can. J. Soil Sci.* **77,** 459–467.

Duff M. C., Hunter D. B., Bertsch P. M., and Amrhein C. (1999) Factors influencing uranium reduction and solubility in evaporation pond sediments. *Biogeochemistry* **45,** 95–114.

Eary L. E. and Rai D. (1988) Chromate removal from aqueous wastes by reduction with ferrous iron. *Environ. Sci. Technol.* **22,** 972–977.

Eng P. J., Rivers M. L., Yang B. X., and Schildkamp W. (1995) Microfocusing 4-keV to 65-keV X-rays with bent Kirkpatrick–Baez mirrors. *SPIE* 41–51.

Fiedor J. N., Bostick W. D., Jarabek R. J., and Farrell J. (1998) Understanding the mechanism of uranium removal from groundwater by zero-valent iron using X-ray photoelectron spectroscopy. *Environ. Sci. Technol.* **32,** 1466–1473.

Francis A. J., Dodge C. J., Lu F. L., Halada G. P., and Clayton C. R. (1994) XPS and XANES studies of uranium reduction by *Clostridium* sp. *Environ. Sci. Technol.* **28,** 636–639.

Fredrickson J. K., Zachara J. M., Kennedy D. W., Dong H., Onstott T. C., Hinman N. W., and Li S. M. (1998) Biogenic iron mineralization accompanying the dissimilatory reduction of hydrous ferric oxide by a groundwater bacterium. *Geochim. Cosmochim. Acta* **62,** 3239–3257.

Gorby Y. A. and Lovley D. R. (1992) Enzymatic uranium precipitation. *Environ. Sci. Technol.* **26,** 205–207.

Greenberg J. and Tomson M. (1992) Precipitation and dissolution kinetics and equilibria of aqueous ferrous carbonate vs. temperature. *Appl. Geochem.* **7,** 185–190.

Grenthe I., Fuger J., Konings R. J. M., Lemire R. J., Muller A. B., Nguyen–Trung Cregu C., and Wanner H. (1992a) *Chemical Thermodynamics Uranium*. Elsevier Science.

Grenthe I., Stumm W., Laaksuharju M., Nilsson A.-C., and Wikberg P. (1992b) Redox potential and redox reactions in deep groundwater systems. *Chem. Geol.* **98,** 131–150.

Grenthe I., Sandino M. C. A., Puidomenech I., and Rand M. H. (1995) Corrections to the uranium NEA–TDB review. In *Chemical Thermodynamics of Americium* (eds. R. A. Silva, G. Bidoglio, M. Rand, P. B. Robouch, H. Wanner, and I. Puigdomenech), pp. 347–374. Elsevier Science.

Gu B., Liang L., Dickey M. J., Yin X., and Dai S. (1998) Reductive precipitation of uranium(VI) by zero-valent iron. *Environ. Sci. Technol.* **32,** 3366–3373.

Haderlein S. B. and Pecher K. (1999) Pollutant reduction in heterogeneous Fe(II)-Fe(III) systems. In *Mineral–Water Interfacial Reactions: Kinetics and Mechanisms*, Chapter 17 (eds. D. L. Sparks and T. J. Grundl), pp. 342–356. Am. Chem. Soc.

Heron G., Crouzet C., Bourg A. C. M., and Christensen T. H. (1994a) Speciation of Fe(II) and Fe(III) in contaminated aquifer sediments using chemical extraction techniques. *Environ. Sci. Technol.* **28,** 1698–1705.

Heron G., Tjell J. C., and Christensen T. H. (1994b) Oxidation capacity of aquifer sediment. In *Hydrocarbon Bioremediation.* (eds. R. E. Hinchee, B. C. Alleman, R. E. Hoeppel, and R. N. Miller), pp. 278–284. Lewis Publishers.

Hocking W. H., Shoesmith D. W., and Betteridge J. S. (1992) Reactivity effects in the oxidative dissolution of UO_2 nuclear fuel. *J. Nucl. Mater.* **190,** 36–45.

Hsi C.-K. and Langmuir D. (1985) Adsorption of uranyl onto ferric oxyhydroxides: Application of the surface complexation site-binding model. *Geochim. Cosmochim. Acta* **49,** 1931–1941.

Hunter D. B. and Bertsch P. M. (1998) In situ examination of uranium contaminated soil particles by micro-X-ray absorption and microfluorescence spectroscopies. *J. Radioanal. Nucl. Chem.* **234,** 237–242.

Kieft T. L., Fredrickson J. K., Onstott T. C., Gorby Y. A., Kostandarithes H. M., Bailey T. J., Kennedy D. W., Li S. W., Plymale A. E., Spadoni C. M., and Gray M. S. (1999) Dissimilatory reduction of Fe(III) and other electron acceptors by a *Thermus* isolate. *Appl. Environ. Microbiol.* **65,** 1214–1221.

Klausen J., Tröber S. P., Haderlein S. B., and Schwarzenbach R. P. (1995) Reduction of substituted nitrobenzenes by Fe(II) in aqueous mineral suspensions. *Environ. Sci. Technol.* **29,** 2396–2404.

Kostka J. E. and Nealson K. H. (1995) Dissolution and reduction of magnetite by bacteria. *Environ. Sci. Technol.* **29,** 2535–2540.

Langmuir D. (1978) Uranium solution–mineral equilibria at low temperatures with applications to sedimentary ore deposits. *Geochim. Cosmochim. Acta* **42,** 547–569.

Langmuir D. (1997) *Aqueous Environmental Geochemistry*. Prentice Hall.

Liger E., Charlet L., and Van Cappellen P. (1999) Surface catalysis of uranium(VI) reduction by Fe(II). *Geochim. Cosmochim. Acta* **63,** 2939–2955.

Liu S. V., Zhou J., Zhang C., Cole D. R., Gajdarziska–Josifovska M., and Phelps T. J. (1997) Thermophilic Fe(III)-reducing bacteria from the deep subsurface: The evolutionary implications. *Science* **277,** 1106–1109.

Liu Y., Fredrickson J. K., Gorby Y. A., Wildung R. E., Balkwill D. L., Ringelberg D., Taylor W. H., and Boone D. R. (1999) Isolation and characterization of new strains of *Shewanella putrefaciens* from the terrestrial subsurface. *Appl. Environ. Microbiol.* (submitted).

Lonergan D. J., Jenter H. L., Coates J. D., Phillips E. J. P., Schmidt T. M., and Lovley D. R. (1996) Phylogenetic analysis of dissimilatory Fe(III)-reducing bacteria. *J. Bacteriol.* **178,** 2402–2408.

Lovley D. R. (1991) Dissimilatory Fe(III) and Mn(IV) reduction. *Microbiol. Rev.* **55,** 259–287.

Lovley D. R. (1995) Bioremediation of organic and metal contaminants with dissimilatory metal reduction. *J. Indust. Microbiol.* **14,** 85–93.

Lovley D. R., Chapelle F. H., and Phillips E. J. P. (1990) Fe(III)-reducing bacteria in deeply buried sediments of the Atlantic Coastal Plain. *Geology* **18,** 954–957.

Lovley D. R., Coates J. D., Blunt–Harris E. L., Phillips E. J. P., and Woodward J. C. (1996) Humic substances as electron acceptors for microbial respiration. *Nature* **382,** 445–448.

Lovley D. R., Fraga J. L., Blunt–Harris E. L., Hayes L. A., Phillips E. J. P., and Coates J. D. (1998) Humic substances as a mediator for microbially catalyzed metal reduction. *Acta Hydrochim. Hydrobiol.* **26,** 152–157.

Lovley D. R. and Phillips E. J. P. (1988) Novel mode of microbial energy metabolism: Organic carbon oxidation coupled to dissimilatory reduction of iron or manganese. *Appl. Environ. Microbiol.* **54,** 1472–1480.

Lovley D. R. and Phillips E. J. P. (1992a) Bioremediation of uranium contamination with enzymatic uranium reduction. *Environ. Sci. Technol.* **26,** 2228–2234.

Lovley D. R. and Phillips E. J. P. (1992b) Reduction of uranium by *Desulfovibrio desulfuricans. Appl. Environ. Microbiol.* **58,** 850–856.

Lovley D. R., Phillips E. J. P., Gorby Y. A., and Landa E. R. (1991) Microbial reduction of uranium. *Nature* **350,** 413–416.

Lovley D. R., Roden E. E., Phillips E. J. P., and Woodward J. C. (1993) Enzymatic iron and uranium reduction by sulfate-reducing bacteria. *Marine Geol.* **113,** 41–53.

McKee B. A. and Todd J. F. (1993) Uranium behavior in a permanently anoxic fjord: microbial control? *Limnol. Oceanogr.* **38,** 408–414.

Mohagheghi A., Updegraff D. M., and Goldhaber M. B. (1985) The role of sulfate-reducing bacteria in the deposition of sedimentary uranium ores. *Geomicrobiol. J.* **4,** 153–173.

Morel F. M. M. (1983) *Principles of Aquatic Chemistry*. John Wiley & Sons.

Morris D. E., Allen P. G., Berg J. M., Chisholm–Brause C. J., Conradson S. D., Donohoe R. J., Hess N. J., Musgrave J. A., and Tait C. D. (1996) Speciation of uranium in Fernald soils by molecular spectroscopic methods: Characterization of untreated soils. *Environ. Sci. Technol.* **30,** 2322–2331.

Myers C. and Myers J. (1997) Outer membrane cytochromes of *Shewanella putrefaciens* MR-1: Spectral analysis, and purification of the 83-kDa *c*-type cytochrome. *Biochim. Biophys. Acta* **1326,** 307–318.

Myers J. M. and Myers C. R. (1998) Isolation and sequence of *omcA*, a gene encoding a decaheme outer membrane cytochrome *c* of *Shewanella putrefaciens* MR-1, and detection of *omcA* homologs in other strains of *S. putrefaciens. Biochim. Biophys. Acta* **1373,** 237–251.

Myers C. R. and Nealson K. H. (1988) Bacterial manganese reduction and growth with manganese oxide as the sole electron acceptor. *Science* **240,** 1319–1321.

Olsen S. R. and Sommers L. E. (1982) Phosphorous. In *Methods of Soil Analysis, Part 2- Chem. and Microbiological Properties* (eds. A. L. Page, R. H. Miller, and D. R. Keeney), pp. 403–430. Am. Soc. Agronomy.

Peterson M. L., White A. F., Brown Jr.G. E., and Parks G. A. (1997) Surface passivation of magnetite by reaction with aqueous Cr(VI): XAFS and TEM results. *Environ. Sci. Technol.* **31,** 1573–1576.

Phillips E. J. P., Landa E. R., and Lovley D. R. (1995a) Remediation of uranium contaminated soils with bicarbonate extraction and microbial U(VI) reduction. *J. Industrial Microbiol.* **14,** 203–207.

Phillips P., Bender J., Simms R., Rodriguezeaton S., and Britt C. (1995b) Manganese removal from acid coal-mine drainage by a pond containing green algae and microbial mat. *Water Sci. Technol.* **31,** 161–170.

Roden E. E. and Zachara J. M. (1996) Microbial reduction of crystalline Fe(III) oxides: Influence of oxide surface area and potential for cell growth. *Environ. Sci. Technol.* **30,** 1618–1628.

Rugge K., Hofstettler T. B., Haderlain S. B., Bjer P. L., Knudsen S., Zraunig C., Mosbek H., and Christensen T. H. (1998) Characterization of predominant reductants in an anaerobic leachate-contaminated aquifer by nitroaromatic probe compounds. *Environ. Sci. Technol.* **32,** 23–31.

Sandino M. C. A. and Grambow B. (1994) Solubility equilibria in the U(VI)–Ca–K–Cl–H_2O system: Transformation of schoepite into becquerelite and compreignacite. *Radiochim. Acta* **66,** 37–43.

Savitzky A. and Golay M. J. E. (1964) Smoothing and differentiation of data by simplified least squares procedures. *Anal. Chem.* **36,** 1627–1639.

Schwertmann U. and Cornell R. M. (1991) *Iron Oxides in the Laboratory: Preparation and Characterization*. VCH.

Scott D. T., McKnight D. M., Blunt–Harris E. L., Kolesar S. E., and Lovley D. R. (1998) Quinone moieties act as electron acceptors in the reduction of humic substances by humics-reducing microorganisms. *Environ. Sci. Technol.* **32,** 2984–2989.

Scott M. J. and Morgan J. J. (1990) Energetics and conservative properties of redox systems. In *Chem. Modeling of Aqueous Systems II* (eds. D. C. Melchior and R. L. Bassett), Chap. 29, pp. 368–378. Am. Chem. Soc.

Shoesmith D. W., Sunder S., Bailey M. G., and Wallace G. J. (1989) The corrosion of nuclear fuel (UO_2) in oxygenated solutions. *Corrosion Sci.* **29,** 1115–1128.

Smith J. V. and Rivers M. L. (1995) Synchrotron X-ray microanalysis. In *Microprobe Techniques in the Earth Sciences* (eds. P. J. Potts, J. F. W. Bowles, S. J. B. Reed, and M. R. Cave), pp. 163–233. Chapman & Hall.

Smith R. M. and Martell A. E. (1997) *NIST Critically Selected Stability Constants of Metal Complexes Database. Version 30, User's Guide and Database Software*. NIST Standard Reference Database 46.

Sowder A. G., Clark S. B., and Fjeld R. A. (1996) The effect of silica and phosphate on the transformation of schoepite to becquerelite and other uranyl phases. *Radiochim. Acta* **74,** 45–49.

Stookey L. L. (1970) Ferrozine—a new spectrophotometric reagent for iron. *Anal. Chem* **42,** 779–781.

Stumm W. (1992) Redox processes mediated by surfaces. In *Chemistry of the Solid–Water Interface* (ed. W. Stumm), pp. 309–335. John Wiley and Sons.

Sunder S., Shoesmith D. W., Christensen H., and Millers N. H. (1992) Oxidation of UO_2 fuel by the products of gamma radiolysis of water. *J. Nucl. Mater.* **190,** 78–86.

Taylor P. T., Wood D. D., and Owen D. G. (1991) Crystallization of U_3O_8 and hydrated UO_3 on UO_2 fuel in aerated water near 200°C. *J. Nuclear Mater.* **183,** 105–114.

Tsapin A. I., Nealson K. H., Meyers T., Cusanovich M. A., van Beuumen J., Crosby L. D., Feinberg B. A., and Zhang C. (1996) Purification and properties of a low-redox-potential tetraheme cytochrome c_3 from *Shewanella putrefaciens. J. Bacteriol.* **178,** 6386–6388.

Vochten R. and Van Haverbeke L. (1990) Transformation of schoepite into uranyl oxide hydrates: Becquerelite, billietite and wolsendorfite. *Mineral. Petrol.* **43,** 65–72.

Vochten R., Van Haverbeke L., and Sobry R. (1991) Transformation of schoepite into uranyl oxide hydrates of the bivalent cations Mg^{2+}, Mn^{2+}, and Ni^{2+}. *J. Mater. Chem.* **1,** 637–642.

Waite T. D., Davis J. A., Payne T. E., Waychunas G. A., and Xu N. (1994) Uranium(VI) adsorption to ferrihydrite: Application of a surface complexation model. *Geochim. Cosmochim. Acta* **58,** 5465–5478.

Yang B. X., Rivers M. L., Schildkamp W., and Eng P. (1995) GEOCARS microfocusing Kirkpatrick–Baez mirror bender development. *Rev. Sci. Instrum.* **66,** 2278.

Zachara J. M., Smith S. C., and Fredrickson J. K. (2000). The effect of biogenic Fe(II) on the stability and sorption of Co(II)$EDTA^{2-}$ to goethite and a subsurface sediment. *Geochim. Cosmochim. Acta* **64,** 1345–1362.

Zachara J. M., Fredrickson J. K., Li S. M., Kennedy D. W., Smith S. C., and Gassman P. L. (1998) Bacterial reduction of crystalline Fe(III) oxides in single phase suspensions and subsurface materials. *Am. Mineral* **83,** 1426–1443.

Zehnder A. J. B. and Stumm W. (1988) Geochemistry and biogeochemistry of anaerobic habitats. In *Biology of Anaerobic Microorganisms* (ed. A. J. B. Zehnder), pp. 1–38. John Wiley & Sons.